PCCP

Accepted Manuscript

ROYAL SOCIETY OF CHEMISTRY

www.rsc.org/pccp

Assessing the Performance of MM/PBSA and MM/GBSA Methods. 5. Improved Docking Performance by Using High Solute Dielectric Constant MM/GBSA and MM/PBSA Rescoring

Huiyong Sun[a,b], Youyong Li[a], Mingyun Shen[a], Sheng Tian[a], Lei Xu[b], Peichen Pan[b], Yan Guan[a], and Tingjun Hou[a,b,*]

[a] Institute of Functional Nano and Soft Materials (FUNSOM), Jiangsu Key Laboratory for Carbon-Based Functional Materials and Devices and Collaborative Innovation Center of Suzhou Nano Science and Technology, Soochow University, Suzhou, Jiangsu 215123, P. R. China.

[b]College of Pharmaceutical Sciences, Zhejiang University, Hangzhou, Zhejiang 310058, China

Corresponding author:

Tingjun Hou

E-mail: tingjunhou@zju.edu.cn or tingjunhou@hotmail.com

Phone: +86-512-65882039

Keywords: MM/GBSA, MM/PBSA, MD simulation, Virtual Screening, Dielectric Constant

For Table of Contents Use Only

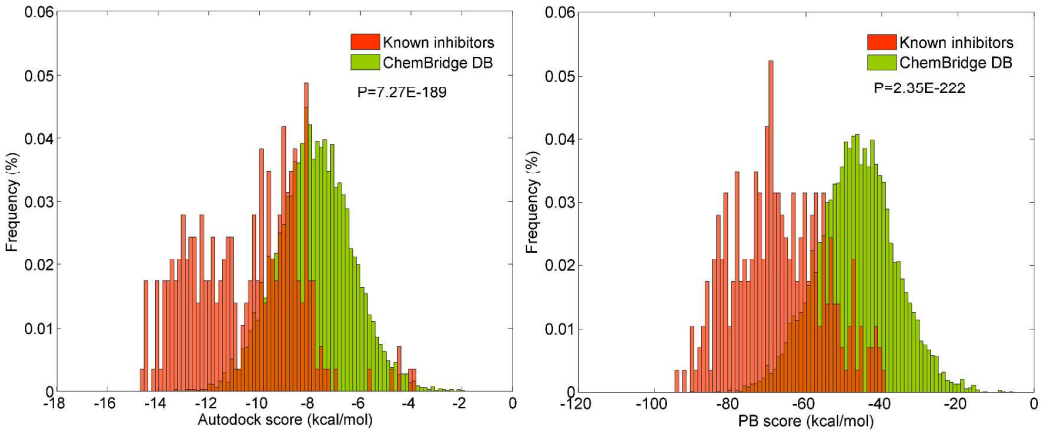

Running Title: The docking performance can be markedly improved by using a relatively higher interior dielectric constant MM/GBSA or MM/PBSA rescoring strategy.

Abstract

With the rapid development of computational technique and hardware, more rigorous and precise theoretical models have been used to predict the binding affinities of a large number of small molecules to a biomolecule. By employing continuum solvation models, the MM/GBSA and MM/PBSA methodologies achieve good balance between low computational cost and reasonable prediction accuracy. In this study, we have thoroughly investigated the effects of interior dielectric constant, molecular dynamics (MD) simulation, and the number of top-scored docking poses on the performance of the MM/GBSA and MM/PBSA rescoring of docking poses for three tyrosine kinases, including ABL, ALK, and BRAF. Overall, the MM/PBSA and MM/GBSA rescoring achieved comparative accuracies based on a relatively higher solute (or interior) dielectric constant (i.e. ε=2, or 4), and could markedly improve the 'screening power' and 'ranking power' given by Autodock. Moreover, with a relatively higher solute dielectric constant, the MM/PBSA or MM/GBSA rescoring based on the best scored docking poses and multiple top-scored docking poses gave similar predictions, implying that much computational cost can be saved with the consideration of the best scored docking poses only. Besides, compared with the rescoring based on the minimized structures, the rescoring based on the MD simulations might not be quite necessary due to its negligible impact on the docking performance. Considering the much higher computational demand of MM/PBSA, MM/GBSA with a high solute dielectric constant (ε=2 or 4) is recommended to virtual screening of tyrosine kinases.

Introduction

Molecular docking has exhibited unrivaled charm in virtual screening (VS), where scoring functions play the core role in predicting the binding modes and binding affinities of ligands. Three criterions have been used to evaluate how well a scoring function or a docking algorithm works:[1] 'docking power', which evaluates the consistency between the predicted binding pose and the experimental structure of a ligand. A reproduced RMSD (root-mean-square deviation) less than 2.0 Å is usually thought as a successful docking; 'screening power', which evaluates the capability of molecular docking to distinguish the inhibitors from non-inhibitors of a target. The *p*-value of student's *t*-test or/and AUC value (area under curve) of ROC curve (receiver operating characteristic curve) are usually used for this evaluation; and 'ranking power', which evaluates the correlation between the predicted binding affinities and the experimental data, and Pearson and Spearman correlations are commonly used for this assessment.

Numerous scoring functions with relatively high precision have been developed, i.e. the scoring functions of PLP,[2] Rosetta,[3] Glide,[4] and Autodock,[5] and successfully used in various studies,[6-8] However, in order to achieve a good balance between prediction accuracy and computational efficiency, approximations were introduced in most docking scoring functions, which often impair the accuracy of predictions. Considering a database for VS usually has a great number of molecules, improving only 1% of the docking accuracy will markedly decrease the false positive rate.

Compared with most scoring functions used in molecular docking, the MM/GBSA (Molecular Mechanics/Generalized Born Surface Area) and MM/PBSA (Molecular Mechanics/Poisson Boltzmann Surface Area) methodologies employ more rigorous solvation models, and allow for the decomposition of free energy into contributions originating from different interaction groups.[9-15] Certainly, the MM/GBSA or MM/PBSA calculations based on molecular dynamics (MD) simulations or only molecular mechanics (MM) minimizations are more time-consuming than most scoring functions. However, with the rapid advance of

computer hardware, it is feasible to use MM/GBSA or MM/PBSA as a scoring function in molecular docking calculations or even docking-based VS. In fact, previous studies have evaluated the performance of MM/GBSA or/and MM/PBSA as scoring functions in molecular docking or VS. For example, Brown *et al.* have used MM/PBSA to predict the binding potencies of 308 small molecules targeting three proteins and found significant correlation (r=0.72~0.83) to experimentally measured data.[16] Sgobba and colleagues reported an assessment study of MM/GBSA and MM/PBSA on six drug targets, and they found that MM/PBSA and MM/GBSA could give higher enrichment factors than the docking scoring functions but rescoring based on multiple protein conformations were not necessary for most cases.[17] Zhang *et al.* have done a comprehensive study on the DUD dataset by using MM/GBSA, and summarized that using the top-5 originally scored docking poses for the MM/GBSA rescoring may be a good balance between computational burden and prediction accuracy.[18] However, we will show below that the influence whether to use the best scored docking pose or the best of the top-3 docking poses is not significant when a higher interior dielectric constant (i.e. ε=2 or 4) was used. Besides, we have evaluated the performance of the MM/GBSA and MM/PBSA approaches on the prediction of ligand binding modes ('docking power'), and found that MM/GBSA was superior to most of the widely used scoring functions when the interior dielectric constant of 2 was used.[19] However, it remains unknown whether the interior dielectric constant and MD simulations have marked impacts on the performance of MM/GBSA and MM/PBSA on VS ('screening power'). Therefore, in this study, we evaluated the impacts of interior dielectric constant, MD simulations, and the number of top-scored docking poses on the performance of the MM/GBSA and MM/PBSA rescoring. To our knowledge, this is the first attempt to analyze the performance of the MM/GBSA or MM/PBSA rescoring on VS by using different interior dielectric constant and MD simulations.

Materials and Methods

Dataset Preparation

Three tyrosine kinases were used for the rescoring evaluation, namely ABL (Abelson tyrosine kinase), ALK (Anaplastic lymphoma kinase), and BRAF (v-Raf murine sarcoma viral oncogene homolog B). The known inhibitors of these targets with $IC_{50} \leq 10{,}000$ nM were obtained from the BindingDB database.[20] The numbers of the known inhibitors for ABL, ALK, and BRAF are 286, 342, and 402, respectively. 7000 compounds were used as the chemical background space or non-inhibitors, and they were randomly selected from the Chembridge database based on the similarity of the FCFP_4 fingerprint by using the *Find Diverse Molecules* module in Discovery Studio 2.5. The ratio of the inhibitors *versus* non-inhibitors are 1:24, 1:20, and 1:17 for ABL, ALK, and BRAF, respectively. The protonation states of the small molecules at pH=7.0 were determined by using the *LigPrep* module in Schrödinger version 9.0.

Molecular Docking

The 3D coordinates of the X-ray crystal complexes of ABL,[21-27] ALK,[28-31] and BRAF[32-35] were downloaded from the RCSB protein data bank (PDB). The protonation states of the proteins were determined by using PROPKA (version 3.1).[36] Before molecular docking, the proteins were prepared by using the *Structure Preparation Tool* module in Sybyl-X1.1, which added hydrogen atoms, repaired side-chains of incomplete residues, and optimized the steric hindrance of side-chains. Missing residues were built by using the *Protein Loops* module in Sybyl-X1.1. Autodock4 atomic radii were assigned to the macromolecules. The non-polar hydrogen atoms were merged into the connected heavy atoms to match the Autodock algorithm. The small molecules were docked into each target with Autodock 4.2 program[5] by using the Lamarckian genetic algorithm (LGA).[37] The Gasteiger partial charge[38] was applied to the macromolecules and small molecules for the reason that it could reproduce approximate 80% of the crystallized binding poses of the co-crystallized ligands in the conjunction with Autodock 4.2 scoring function.[39, 40] The grid spacing was set to 0.375 Å with box size of 50 × 50 × 50 centered in the active pocket. Each molecule was docked for 10 times and the top-3 docking poses

associated with the lowest binding affinities were saved for the MM/GBSA and MM/PBSA rescoring calculations.

Structural Optimization and Molecular Dynamics Simulation

Each protein-ligand complex predicted by molecular docking was optimized and rescored by MM/GBSA and MM/PBSA. Then, for each target, 720 systems (~10% of the total systems) with the top MM/GBSA scores were submitted to MD simulations to evaluate the impact of MD on the rescoring accuracy. Before the MM/GBSA and MM/PBSA rescoring, each protein-ligand complex was prepared with the standard procedure in Amber12 simulation package.[41] Due to the reasonable computational efficiency and good performance in binding free energy predictions,[42] the AM1-BCC charges (AM1 with bond charge corrections)[43] of each small molecule were computed by the *sqm* program[44] in AMBER12. The Amber03[45] and GAFF[46] (general Amber force field) force fields were used for the proteins and small molecules, respectively. The counter-ions, Na^+ or Cl^-, were added to neutralize the unbalanced charges in the complexes. For each complex, octahedral TIP3P water box[47] was added with 5 Å out of the solute to reduce the high computational demand.

In the phase of minimization, each complex was minimized for 1000 cycles (500 cycles of steepest descent and 500 cycles of conjugate gradient minimization) and the backbone heavy atoms in each protein were constrained with the elastic constant of 50 kcal/mol·Å^2; then, the constrains for the backbone heavy atoms were reduced to 10 kcal/mol·Å^2 and the other atoms were free to move (500 cycles of steepest descent and 500 cycles of conjugate gradient minimization); and finally, each system was optimized for 3000 cycles without any constrain (1000 cycles of steepest descent and 2000 cycles of conjugate gradient minimization). A cutoff of 8 Å was used to handle the short-range interactions (electrostatic and van der Waals interactions), and the Particle mesh Ewald (PME) algorithm was employed to deal with the long-range electrostatic interactions.[48]

In the MD simulation process, all the covalent bonds involving hydrogen atoms were constrained by using the SHAKE algorithm,[49] and the time step was set to 2 fs.

To prevent the drifting of each protein-ligand complex in the relatively small water box, slight restrains (0.1 kcal/mol·Å^2) were added to the C_α atoms of the N-terminal and C-terminal residues in each protein. Each system was gradually heated from 0 to 300 K during a period of 50 ps in the NVT ensemble, and then equilibrated for 50 ps in the NPT ensemble (T = 300 K and P = 1 atm). At last, a 500 ps production run in the NPT ensemble was performed for each system with the collection interval of 10 ps, and 50 frames were collected for the following MM/GBSA and MM/PBSA rescoring.

MM/GBSA and MM/PBSA Rescoring

The MM/GBSA or MM/PBSA rescoring was carried out for each system based on the minimized structure or the MD trajectory, whereby the free energy of binding is approximated through[12, 13, 50]:

$$\Delta G_{bind} = G_{com} - (G_{rec} + G_{lig}) \quad (1)$$

$$\Delta G_{bind} = \Delta H - T\Delta S \approx \Delta E_{MM} + \Delta G_{sol} - T\Delta S \quad (2)$$

$$\Delta E_{MM} = \Delta E_{internal} + \Delta E_{electrostatic} + \Delta E_{vdw} \quad (3)$$

$$\Delta G_{sol} = \Delta G_{PB/GB} + \Delta G_{SA} \quad (4)$$

$$\Delta G_{SA} = \gamma \Delta A + b \quad (5)$$

where ΔG_{bind} denotes the total free energy change between the bound-state (G_{com}) and unbound-state systems ($G_{rec} + G_{lig}$), and it can be decomposed into three terms: ΔE_{MM}, known as gas-phase interaction energy, which contains electrostatic ($\Delta E_{electrostatic}$) and van der Waals (ΔE_{vdw}) interactions; ΔG_{sol}, solvation energy, which includes the polar ($\Delta G_{PB/GB}$) and non-polar (ΔG_{SA}) components; and $-T\Delta S$, the change of the conformational entropy upon ligand binding, which was not considered here due to the very high computational cost and low prediction accuracy.[51, 52] In this study, the modified GB model developed by Onufriev[53] (GB^{OBC1}) and the PB model developed by Tan and Luo (noted as PB^{pbsa} in Amber12)[54, 55] were employed for the MM/GBSA and MM/PBSA calculations, respectively, due to the fact that they performed better than the other GB (GB^{HTC} and GB^{OBC2}) or PB (PB^{Delphi}) models in our previous

studies.[42, 51] It is well known that the interior (solute) dielectric constant can significantly affect the accuracy (Pearson correlation coefficient and Spearman ranking coefficient) of the investigated systems.[56] Thus, it will be necessary to evaluate the impact of the dielectric constant on the rescoring accuracy. Here, the interior dielectric constant of 1, 2, or 4 was used for both the polar solvation energy (ΔG_{GB} and ΔG_{PB}) rescoring assessment. The solvent (exterior) dielectric constant was set to 80. The non-polar part of the solvation energy (ΔG_{SA}) was estimated by using the LCPO algorithm,[57] where γ and b were set to 0.0072 and 0, respectively, as shown in eq. (5).

Each docking pose was first rescored by MM/GBSA and MM/PBSA based on the minimized structure (the final structure derived from the three-stage optimization), and then, rescored by MM/GBSA and MM/PBSA based on the 50 snapshots extracted from the MD trajectory (for the top 720 systems of each target).

Statistics and Analyses

In this study, the *p*-value for the two distributions of the predicted binding affinities of the known inhibitors and non-inhibitors given by student's *t*-test and the AUC value (area under curve) of ROC (receiver operating characteristic) plot were employed to measure the 'screening power' or 'discrimination power' of molecular docking and MM/GBSA(PBSA) rescoring. The Pearson correlation coefficient was employed to evaluate the 'ranking power' to the known inhibitors of each target. The inhibitor enrichment was used to evaluate the proportion of known inhibitors to the top hits, i.e. the number of known inhibitors found in top 500 hits could be calculated by $N_{inhibitor}/500$.

Results and Discussion

How does the dielectric constant affect the rescoring accuracy of MM/GBSA and MM/PBSA calculations?

To test the 'docking power' of Autodock, the X-ray bound structure of each ligand

was docked back into its corresponding protein structure. The RMSD between each predicted binding pose and the corresponding experimental structure was calculated, and RMSD ≤ 2.0 Å was used as the criterion of successful docking. As shown in Table S1, most of the crystal structures could be well reproduced except 4FOC (ALK, RMSD = 2.25 Å) and 4E26 (BRAF, RMSD = 4.43 Å). Therefore, in the consideration of the RMSD values and the resolutions of the crystal structures, the following three PDB structures, including 2HYY (RMSD: 0.25 Å, resolution: 2.40 Å), 3LCS (RMSD: 0.91 Å, resolution: 1.95 Å), and 3IDP (RMSD 0.54 Å, resolution: 2.70 Å), were selected for ABL, ALK, and BRAF, respectively, to the rescoring evaluation.

Interior dielectric constant exhibits strong regulatory capability in fitting and ranking the ligand binding affinities in condense phase.[19, 51, 58] Several studies have investigated the performance of MM/GBSA or MM/PBSA in VS,[16-18] but they did not explore the impact of interior dielectric constant on rescoring accuracies (only using the default ε=1 for the evaluation). In some cases, based on ε=1, the much time-consuming rescoring even performs worse than the original scoring function.[18]

As shown in Table I, based on the dielectric constant of 1, the accuracies (AUC and *p*-value) of the MM/PBSA and MM/GBSA rescoring are even worse than those of Autodock for ABL (AUC=0.781 for MM/PBSA *versus* 0.859 for Autodock) and ALK (AUC=0.830 for MM/PBSA *versus* 0.898 for Autodock). However, this situation could be substantially improved by using an interior dielectric constant of 2 or 4. As listed in Table I, for ABL, when ε=4 was used, the AUC values of the MM/GBSA and MM/PBSA rescoring are 0.897 and 0.898, respectively, and for ALK, when ε=2 was used, the AUC values of the MM/GBSA and MM/PBSA rescoring are 0.917 and 0.911, respectively. Moreover, in terms of the *p*-values, the MM/GBSA or MM/PBSA rescoring also shows better capability to distinguish the inhibitors from non-inhibitors than molecular docking for the studied systems. The *p*-values of MM/GBSA based on ε=2 are 2.00×10^{-225} and 1.30×10^{-231}, respectively, for ABL and ALK, which are much lower than those of Autodock (7.27×10^{-189} and 9.65×10^{-181}). By averaging the AUC values of the investigated targets in Table I, it is found that the MM/GBSA and MM/PBSA rescoring give comparative accuracies based on the interior dielectric

constant of 2 (0.8818 *versus* 0.8827) and 4 (0.8818 *versus* 0.8863), implying that, in terms of discrimination accuracy, both MM/GBSA and MM/PBSA can be equally used in VS. However, considering the relatively higher computational cost of MM/PBSA, MM/GBSA may be a better choice for VS.

As been discussed above, a relatively higher dielectric constant (2 or 4) was preferred to VS for the studied tyrosine kinases, which may be attributed from the highly charged binding pockets of the tyrosine kinases. As shown in Figure 1, three conserved polar residues (Lys, Glu, and Asp) are crowded in the binding pocket, and form an electrostatic interaction network to execute its catalytic functions to their substrate i.e. ATP. As recommended by our previous study,[51] for the macromolecules with highly-charged binding interface, higher ε_{in} values are preferred to accurately consider electronic polarization effect. This finding is also consistent with our another study on 118 crystallized bound-state tyrosine kinases (SCOP ID: d.144.1.7), which showed that the use of a dielectric constant of 4 could give a better Pearson correlation for the predicted binding affinities.[56] Taken together, our study demonstrates that the MM/GBSA or MM/PBSA rescoring indeed improves the discrimination or screening power. Certainly, the rescoring performance is quite sensitive to solute dielectric constant, and a relatively higher solute dielectric constant is preferred to the studied systems.

Should multiple docking poses be used for MM/GBSA and MM/PBSA rescoring?

It is well known that the docking poses of the same ligand predicted by two scoring functions may be not consistent. Our previous study shows that the correct binding structures for some systems were not the best-scored conformations predicted by the popular scoring functions used in molecular docking, but could be found in the top-3 scored conformations predicted by Autodock.[19] Therefore, in this study, the top-3 scored docking poses for each system were rescored by MM/PBSA or MM/GBSA. As shown in Figure 2, based on the best of the three rescored poses (green bars), the AUC values are all higher than the corresponding rescored results based on the best scored docking poses (red bars), suggesting that the MM/GBSA or MM/PBSA rescoring

based on multiple docking poses improves the screening power than that only based on the best scored docking poses. However, the increase ratio of AUC is dependent with the interior dielectric constant. When the interior dielectric constant of 1 was used, the ΔAUCs between the AUCs derived from the best of the top-3 scored docking poses and the best scored docking pose are large, and the average ΔAUCs of MM/GBSA and MM/PBSA are 0.0117 and 0.0175, respectively (Table II), which are on the same magnitude of the AUC difference between the AUCs given by Autodock and MM/PBSA(GBSA) (0.02~0.04, Table I).

However, the ΔAUCs begin to decrease when a higher interior dielectric constant was employed, and the average ΔAUCs decrease to 0.0020 and 0.0037 for MM/GBSA and MM/PBSA, respectively, at the interior dielectric constant of 4, implying that the influence of the use of multiple docking poses for rescoring is not significant. The deep reason has been revealed by analyzing the difference of the Pearson correlation coefficients between the docking results (Pearson correlation coefficient of the docking results) and the rescoring results (Pearson correlation coefficient of the MM/GBSA and MM/PBSA results based on the interior dielectric constant of 1, 2, or 4). As shown in Figure 3, strong negative correlations are observed between the ΔAUC (AUC difference between using the best scored pose and using the best of the top-3 scored poses rescored by MM/PBSA(GBSA)) and Δr (difference of the Pearson correlation coefficients between the docking accuracy and the MM/PBSA(GBSA) accuracy), implying that the ΔAUC (AUC difference between using the best scored pose and using the best of the top-3 scored poses) decreases with the increase of the Pearson correlation coefficient. That is to say, good ranking of a rescoring function can avoid choosing the best pose from the multiple scored poses.

As shown in Table III, all the investigated systems achieve the best Pearson correlation coefficients at the interior dielectric constant of 4 for both the MM/GBSA and MM/PBSA calculations. Therefore, it can be summarized that, for the studied systems, based on a relatively higher interior dielectric constant, the accuracy of rescoring can be improved, and on the other hand, much computational cost can be saved because multiple docking poses are not necessary for rescoring.

Impact of the rescoring strategy on enrichment

Enrichment is an important criterion to evaluate whether a theoretical model can effectively discriminate known inhibitors from non-inhibitors. The enrichments of the top 200, 500, and 1000 molecules for each target, which represents the top ~3%, ~7%, and ~14% hits of the total investigated dataset, were derived from the docking results (Autodock in Table IV) and the rescoring results based on the minimized structures and the MD trajectories (GB/PB in Table IV). Overall, the enrichments of the rescoring results are markedly increased compared with those of the Autodock results. On average, the enrichments are improved about 13% (ABL) ~ 33% (BRAF) for the top 500 molecules, and about 8% (ABL) ~ 26% (BRAF) for the top 1000 molecules based on the minimized structures (except for the MM/PBSA enrichments based on ε=1 for ABL and ALK, which are worse than those based on the Autodock scores). For ABL, the enrichment of the top 200 investigated molecules is the same or a bit worse than that based on the docking results (with the enrichment change ratio decreased for 4.6% on average), meaning that the rescoring strategy may fail in the most top-scored enrichment adjustment. However, concerning the relatively low correlation coefficients of the top-scored known inhibitors (not more than 0.48 of the Pearson correlation coefficient as shown in Table III), it actually does need to use more broad range of top-scored molecules to get more potential activities, where the most favorable binders may be ranked out of the top predicted molecules.

Moreover, an important issue has been discussed for decades that whether MD simulations in conjunction with free energy calculations could improve the prediction accuracy of molecular docking. Here, we also investigated the enrichment capability of MD simulations on the top 720 systems (ranked by the MM/GBSA results based on ε=2) for each target, which represent approximate 10% of the total investigated systems. As shown in Figure 4, the enrichments of the top 200 (blue line) and 500 (green line) rescored molecules based on the MD simulations are slightly different from those only based on the minimizations. It has been found in our previous study that MD simulation in conjunction with MM/GBSA is capable of adjusting the bad

binding mode and selecting the correct binding pose as the most favorable binding conformation from a serial of generated poses of a ligand (namely, the docking power),[19] but it may contribute little to improve the discrimination capability (ranking a variety of small molecules, namely, the screening power) for a large dataset. Besides, MD simulations may do little to improve the correlation coefficient of the investigated systems. As illustrated in Table V, the Pearson correlation coefficients of the known inhibitors based on the MD simulations are even worse than those based on the minimized structures for the targets of ABL and ALK, which is consistent with our previous study that MD simulations may be helpless for the adjustment of prediction accuracy.[56] Thereby, due to the finite-precise theoretical models and the exponentially increased computational time, it may be not necessary to incorporate MD simulations to VS at this stage.

Why MM/GBSA and MM/PBSA are capable of improving the docking performance?

The rescoring strategy by using MM/GBSA or MM/PBSA has exhibited undefeatable advantage than the Autodock algorithm to not only the 'screening power' but also the 'ranking power'. As shown in Figure 5, some known inhibitors of ABL are found to have very unfavorable binding affinities compared with some other inhibitors and most of the non-inhibitors by using the Autodock algorithm, such as the red bars located at -6~-4 kcal/mol of the Autodock scores (Figure 5A1) where two inhibitors are not shown in Figure 5A1 due to the unreasonably unfavorable binding affinities of 30.30 kcal/mol and 727.25 kcal/mol. However, the distribution can be changed by using the MM/GBSA and MM/PBSA methodologies, as shown in Figures 5A2 and 5A3, where no inhibitor tails was found in the distributions of the inhibitors. Similarly, the peaks between the known inhibitors and non-inhibitors cannot be effectively discriminated by using the Autodock scoring function for BRAF (Figure 5C1). However, the peaks could be apparently discriminated by the MM/PBSA rescored results, as illustrated in Figure 5C3.

For the 'ranking power', most of the investigated protocols, such as MM/GBSA

based on ε=1, 2, 4, have shown increased correlations to Autodock (Table III, expect for the MM/PBSA results of ALK based on ε=1), suggesting that the complicated scoring models indeed have the advantage in VS. As mentioned above, to make the Figures and Tables looked normal, two inhibitors with much unfavorable binding affinities to ABL were eliminated. However, as shown in Figure 6A, the correlation between the experimental data and the Autodock results of ABL becomes very strange when incorporating the two inhibitors. One inhibitor, surrounded by pink shadow in Figure 6A, exhibits very positive predicted binding affinity (>700 kcal/mol) to ABL and thus results in very low Pearson correlation coefficient of the docking results (r_p=0.077±0.007). However, the binding affinity of the inhibitor can be adjusted to ~-88 kcal/mol by using the MM/GBSA approach as shown in pink shadow in Figure 6B, and no point goes apparently out of the relative region either, leading to the remarkable improvement of the Pearson correlation (r_p=0.322±0.007). Besides, the low correlations between the docking results and the best rescored results (ABL, r_p=0.698 for the 284 inhibitors and r_p=0.060 for the 286 inhibitors (including the two much unfavorable inhibitors), Figure 6E; ALK, r_p=0.550, Figure 6F; and BRAF, r_p=0.574, Figure 6G) means that MM/GBSA and MM/PBSA are indeed capable of readjusting the binding affinities of the existing docking poses ('ranking power').

A deep analysis shows that the MM/GBSA and MM/PBSA approaches in conjunction with the AMBER force field and optimization strategy have adjusted the binding pose to fit the binding site. It should be mentioned that the optimizations of the studied system are quite necessary for the MM/GBSA and MM/PBSA rescoring, because these methodologies originally developed and used for the binding free energy calculations based on the Amber force field are very sensitive to the initial conformations.[59] As shown in Figure 6D, the binding pose of the ligand (yellow) and the neighboring residue Asp381 (green) have been optimized compared with those predicted by docking (Figure 6C). Thus, it can be concluded that the combination of MM/GBSA (MM/PBSA) and MM optimization executes much like 'flexible docking', which can effectively adjust the binding pose and the conformation of the interaction residues around a ligand.

Conclusion

In this study, we have systemically investigated the impacts of interior dielectric constant, MD simulations, and the number of top-scored docking poses on the performance of MM/GBSA and MM/PBSA rescoring in large scale VS. The results can be summarized as follows:

(1) For the investigated kinase systems, a high interior dielectric constant is necessary for improving the rescoring accuracy (in terms of 'screening power') for both MM/GBSA and MM/PBSA , which is consistent with our previous study that in most cases MM/GBSA and MM/PBSA work better with a relatively higher dielectric constant (i.e. ε=2 or 4).[56]

(2) The use of a higher dielectric constant not only improves the discrimination performance of MM/GBSA and MM/PBSA, but may also save much computational cost because high dielectric constant can attenuate the impact of the selection of the top-scored docking poses. That is to say, only using the best-scored docking poses for the rescoring will give comparative accuracy to use the multiple top-scored docking poses.

(3) MD simulations may be unnecessary for improving enrichment, but optimizations are indeed necessary for the MM/GBSA or MM/PBSA rescoring because they can adjust the ligand binding conformation and executes much like a flexible docking.

(4) Although MM/PBSA and MM/GBSA have achieved comparative accuracies at a relatively higher dielectric constant (ε=2 or 4), considering the much higher computational demand of MM/PBSA, MM/GBSA may be a better choice for VS.

Acknowledgment

This study was supported by the National Science Foundation of China (21173156), the National Basic Research Program of China (973 program, 2012CB932600), and the Priority Academic Program Development of Jiangsu Higher Education Institutions

(PAPD).

Supporting information

Table S1. Reproduction of the binding mode of the co-crystallized ligands.

References

1 Y. Li, L. Han, Z. Liu and R. Wang, *J. Chem. Inf. Model.*, 2014, **54**, 1717-1736.

2 D. K. Gehlhaar, G. M. Verkhivker, P. A. Rejto, C. J. Sherman, D. R. Fogel, L. J. Fogel and S. T. Freer, *Chem. Biol.*, 1995, **2**, 317-324.

3 A. Zanghellini, L. Jiang, A. M. Wollacott, G. Cheng, J. Meiler, E. A. Althoff, D. Röthlisberger and D. Baker, *Protein Sci.*, 2006, **15**, 2785-2794.

4 T. A. Halgren, R. B. Murphy, R. A. Friesner, H. S. Beard, L. L. Frye, W. T. Pollard and J. L. Banks, *J. Med. Chem.*, 2004, **47**, 1750-1759.

5 G. M. Morris, R. Huey, W. Lindstrom, M. F. Sanner, R. K. Belew, D. S. Goodsell and A. J. Olson, *J. Comput. Chem.*, 2009, **30**, 2785-2791.

6 C. E. Tinberg, S. D. Khare, J. Dou, L. Doyle, J. W. Nelson, A. Schena, W. Jankowski, C. G. Kalodimos, K. Johnsson and B. L. Stoddard, *Nature*, 2013, **501**, 212-216.

7 L. Xu, Y. Zhang, L. Zheng, C. Qiao, Y. Li, D. Li, X. Zhen and T. Hou, *J. Med. Chem.*, 2014, **57**, 3737-3745.

8 F. Bai, Y. Xu, J. Chen, Q. Liu, J. Gu, X. Wang, J. Ma, H. Li, J. N. Onuchic and H. Jiang, *Proc. Natl. Acad. Sci. USA*, 2013, **110**, 4273-4278.

9 H. Gohlke, C. Kiel and D. A. Case, *J. Mol. Biol.* , 2003, **330**, 891-914.

10 T. Hou, Z. Xu, W. Zhang, W. A. McLaughlin, D. A. Case, Y. Xu and W. Wang, *Mol. Cell Proteomics.*, 2009, **8**, 639-649.

11 T. J. Hou, N. Li, Y. Y. Li and W. Wang, *J. Proteome Res.*, 2012, **11**, 2982-2995.

12 N. Homeyer and H. Gohlke, *Mol. Inf.*, 2012, **31**, 114-122.

13 P. A. Kollman, I. Massova, C. Reyes, B. Kuhn, S. H. Huo, L. Chong, M. Lee, T. Lee, Y. Duan, W. Wang, O. Donini, P. Cieplak, J. Srinivasan, D. A. Case and T. E. Cheatham, *Accounts Chem Res*, 2000, **33**, 889-897.

14 H. Liu, X. Yao, C. Wang and J. Han, *Mol. Pharmaceut.*, 2010, **7**, 894-904.

15 H. Liu and X. Yao, *Mol. Pharmaceut.*, 2009, **7**, 75-85.

16 S. P. Brown and S. W. Muchmore, *J. Med. Chem*, 2009, **52**, 3159-3165.

17 M. Sgobba, F. Caporuscio, A. Anighoro, C. Portioli and G. Rastelli, *Eur. J. Med. Chem.*, 2012, **58**, 431-440.

18 X. Zhang, S. E. Wong and F. C. Lightstone, *J. Chem. Inf. Model.*, 2013, **54**, 324-337.

19 T. J. Hou, J. M. Wang, Y. Y. Li and W. Wang, *J. Comput. Chem.*, 2011, **32**, 866-877.

20 T. Liu, Y. Lin, X. Wen, R. N. Jorissen and M. K. Gilson, *Nucleic Acids Res.*, 2007, **35**, D198-D201.

21 T. Horio, T. Hamasaki, T. Inoue, T. Wakayama, S. Itou, H. Naito, T. Asaki, H. Hayase and T. Niwa, *Bioorg. Med. Chem. Lett.*, 2007, **17**, 2712-2717.

22 N. M. Levinson, O. Kuchment, K. Shen, M. A. Young, M. Koldobskiy, M. Karplus, P. A. Cole and J. Kuriyan, *PLoS biol.*, 2006, **4**, e144.

23 B. Okram, A. Nagle, F. J. Adrián, C. Lee, P. Ren, X. Wang, T. Sim, Y. Xie, X. Wang and G. Xia, *Chem. Biol.*, 2006, **13**, 779-786.

24 S. W. Cowan-Jacob, G. Fendrich, A. Floersheimer, P. Furet, J. Liebetanz, G. Rummel, P. Rheinberger, M. Centeleghe, D. Fabbro and P. W. Manley, *Acta Crystallogr. D Biol. Crystallogr.*, 2006, **63**, 80-93.

25 E. Weisberg, P. W. Manley, W. Breitenstein, J. Brüggen, S. W. Cowan-Jacob, A. Ray, B. Huntly, D. Fabbro, G. Fendrich and E. Hall-Meyers, *Cancer cell*, 2005, **7**, 129-141.

26 N. M. Levinson and S. G. Boxer, *PloS one*, 2012, **7**, e29828.

27 W. W. Chan, S. C. Wise, M. D. Kaufman, Y. M. Ahn, C. L. Ensinger, T. Haack, M. M. Hood, J. Jones, J. W. Lord and W. P. Lu, *Cancer cell*, 2011, **19**, 556-568.

28 R. T. Bossi, M. B. Saccardo, E. Ardini, M. Menichincheri, L. Rusconi, P. Magnaghi, P. Orsini, N. Avanzi, A. L. Borgia and M. Nesi, *Biochemistry*, 2010, **49**, 6813-6825.

29 C. Lee, Y. Jia, N. Li, X. Sun, K. Ng, E. Ambing, M. Gao, S. Hua, C. Chen and S. Kim, *Biochem. J.*, 2010, **430**, 425-437.

30 M. C. Bryan, D. A. Whittington, E. M. Doherty, J. R. Falsey, A. C. Cheng, R. Emkey, R. L. Brake and R. T. Lewis, *J. Med. Chem.*, 2012, **55**, 1698-1705.

31 R. T. Lewis, C. M. Bode, D. M. Choquette, M. Potashman, K. Romero, J. C. Stellwagen, Y. Teffera, E. Moore, D. A. Whittington and H. Chen, *J. Med. Chem.*, 2012, **55**, 6523-6540.

32 J. Tsai, J. T. Lee, W. Wang, J. Zhang, H. Cho, S. Mamo, R. Bremer, S. Gillette, J. Kong and N. K. Haass, *Proc. Natl. Acad. Sci. USA*, 2008, **105**, 3041-3046.

33 L. Ren, S. Wenglowsky, G. Miknis, B. Rast, A. J. Buckmelter, R. J. Ely, S. Schlachter, E. R. Laird, N. Randolph and M. Callejo, *Bioorg. Med. Chem. Lett.*, 2011, **21**, 1243-1247.

34 A. L. Smith, F. F. DeMorin, N. A. Paras, Q. Huang, J. K. Petkus, E. M. Doherty, T. Nixey, J. L. Kim, D. A. Whittington and L. F. Epstein, *J. Med. Chem.*, 2009, **52**, 6189-6192.

35 J. Qin, P. Xie, C. Ventocilla, G. Zhou, A. Vultur, Q. Chen, Q. Liu, M. Herlyn, J. Winkler and R. Marmorstein, *J. Med. Chem.*, 2012, **55**, 5220-5230.

36 C. R. Søndergaard, M. H. Olsson, M. Rostkowski and J. H. Jensen, *J. Chem. Theory Comput.*, 2011, **7**, 2284-2295.

37 G. M. Morris, D. S. Goodsell, R. S. Halliday, R. Huey, W. E. Hart, R. K. Belew and A. J. Olson, *J. Comput. Chem.*, 1998, **19**, 1639-1662.

38 J. Gasteiger and M. Marsili, *Tetrahedron*, 1980, **36**, 3219-3228.

39 X. Hou, J. Du, J. Zhang, L. Du, H. Fang and M. Li, *J. Chem. Inf. Model.*, 2013, **53**, 188-200.

40 H. Y. Sun, F. Q. Ji, L. Y. Fu, Z. Y. Wang and H. Y. Zhang, *J. Chem. Inf. Model.*, 2013, **53**, 3343-3351.

41 D. Case, T. Darden, T. Cheatham III, C. Simmerling, J. Wang, R. Duke, R. Luo, R. Walker, W. Zhang and K. Merz, *University of California, San Francisco*, 2012.

42 L. Xu, H. Y. Sun, Y. Y. Li, J. M. Wang and T. J. Hou, *J. Phys. Chem. B.*, 2013, **117**, 8408-8421.

43 A. Jakalian, D. B. Jack and C. I. Bayly, *J. Comput. Chem.*, 2002, **23**, 1623-1641.

44 R. C. Walker, M. F. Crowley and D. A. Case, *J. Comput. Chem.*, 2008, **29**, 1019-1031.

45 J. Wang, P. Cieplak and P. A. Kollman, *J. Comput. Chem.*, 2000, **21**, 1049-1074.

46 J. Wang, R. M. Wolf, J. W. Caldwell, P. A. Kollman and D. A. Case, *J. Comput. Chem.*, 2004, **25**, 1157-1174.

47 W. L. Jorgensen, J. Chandrasekhar, J. D. Madura, R. W. Impey and M. L. Klein, *J. Chem. Phys.*, 1983, **79**, 926-935.
48 T. Darden, D. York and L. Pedersen, *J. Chem. Phys.*, 1993, **98**, 10089-10092.
49 J. P. Ryckaert, G. Ciccotti and H. J. C. Berendsen, *J. Comput. Phys.*, 1977, **23**, 327-341.
50 J. M. Wang, T. J. Hou and X. J. Xu, *Curr. Comput.-Aided Drug Des.*, 2006, **2**, 287-306.
51 T. J. Hou, J. M. Wang, Y. Y. Li and W. Wang, *J. Chem. Inf. Model.*, 2011, **51**, 69-82.
52 T. Hou and R. Yu, *J. Med. Chem.*, 2007, **50**, 1177-1188.
53 A. Onufriev, D. Bashford and D. A. Case, *Proteins: Struct., Funct., Bioinf.*, 2004, **55**, 383-394.
54 C. Tan, L. Yang and R. Luo, *J. Phys. Chem. B.*, 2006, **110**, 18680-18687.
55 Q. Lu and R. Luo, *J. Chem. Phys.*, 2003, **119**, 11035-11048.
56 H. Sun, Y. Li, S. Tian, L. Xu and T. Hou, *Phys. Chem. Chem. Phys.*, 2014, **16**, 16719-16729.
57 J. Weiser, P. S. Shenkin and W. C. Still, *J. Comput. Chem.*, 1999, **20**, 217-230.
58 T. Yang, J. C. Wu, C. Yan, Y. Wang, R. Luo, M. B. Gonzales, K. N. Dalby and P. Ren, *Proteins: Struct., Funct., Bioinf.*, 2011, **79**, 1940-1951.
59 J. Wang, P. Morin, W. Wang and P. A. Kollman, *J. Am. Chem. Soc.*, 2001, **123**, 5221-5230.

Legend of the Figures

Figure 1. Binding sites of the investigated tyrosine kinases, (A) ABL, (B) ALK, (C) and BRAF. Three conserved polar residues found in the binding pocket (Lys, Glu, and Asp) are colored in (A) green in ABL, (B) blue in ALK (B), and (C) pink in BRAF. The co-crystallized ligands were shown in yellow stick model. Crystal structures of 2HYY (ABL, A), 3LCS (ALK, B), and 3IDP (BRAF, C) were used for the illustrations.

Figure 2. Comparison of the rescoring accuracies (AUC) of the top docking pose (red) and the best of the top three docking poses (green) under different solvation models and interior dielectric constants for (A) ABL, (B) ALK, and (C) BRAF. The corresponding Autodock results for each target are shown in blue dot line to give a comparison.

Figure 3. Pearson correlation coefficients between the difference of AUCs and difference of the Pearson correlation coefficients of the MM/GBSA and MM/PBSA results based on different interior dielectric constants for (A) ABL, (B) ALK, (C) BRAF, and (D) all data used in the three targets.

Figure 4. Enrichment change between the rescored results (MM/GBSA and MM/PBSA) and the original results (Autodock). Enrichment of the top 200, 500, and 1000 molecules were colored in blue, green, and red, respectively, for the three targets, (A) ABL, (B) ALK, and (C) BRAF. The label 'Min, GB1' (or 'MD, PB2') represents the enrichment change calculated with the minimized structure based on MM/GBSA at the interior dielectric constant of 1 (or calculated with the MD trajectory based on MM/PBSA at the interior dielectric constant of 2).

Figure 5. Distributions of the known inhibitors (red) and non-inhibitors randomly

selected from the Chembridge Database (green). The top-scored pose (derived from the three top-scored docking poses) was employed for the MM/GBSA and MM/PBSA rescoring. The interior dielectric constant of 2 was used for ALK and BRAF, and 4 was used for ABL for the GB/PB calculations.

Figure 6. Adjustment of the unfavorable binding mode by using the MM/GBSA and MM/PBSA rescoring strategy (panels A, B, C, and D) and the Pearson correlation coefficients between the top-scored Autodock poses and the best correlated GB/PB poses (panels E, F, and G) for the known inhibitors of the three systems. The best correlated GB/PB scores were calculated by MM/GBSA at the interior dielectric constant of 4 for ABL, and 2 for ALK, and MM/PBSA at the interior dielectric constant of 2 for BRAF. The standard errors were estimated by randomly selecting 80% of the dataset for 100 times.

Table I. Comparison of the rescoring accuracies based on various protocols.

ABL		ε=1	ε=2	ε=4
Top1-GB[a]	P value	5.54×10^{-185}	2.00×10^{-225}	6.60×10^{-224}
	AUC	0.8475 (-0.0116)[d]	0.8897 (0.0306)	0.8974 (0.0383)
Top1-PB[b]	P value	1.12×10-^{97}	1.04×10^{-201}	4.84×10^{-221}
	AUC	0.7809 (-0.0782)	0.8793 (0.0202)	0.8977 (0.0386)
Autodock[c]	P value		7.27×10^{-189}	
	AUC		0.8591	
ALK		ε=1	ε=2	ε=4
Top1-GB	P value	2.95×10^{-221}	1.30×10^{-231}	5.40×10^{-217}
	AUC	0.9039 (0.0059)	0.9172 (0.0192)	0.9130 (0.0150)
Top1-PB	P value	1.02×10^{-129}	1.23×10^{-207}	2.24×10^{-214}
	AUC	0.8297 (-0.0683)	0.9105 (0.0125)	0.9137 (0.0157)
Autodock	P value		9.65×10^{-181}	
	AUC		0.8980	
BRAF		ε=1	ε=2	ε=4
Top1-GB	P value	9.63×10^{-134}	5.38×10^{-149}	1.30×10^{-143}
	AUC	0.8238 (-0.0046)	0.8384 (0.0100)	0.8349 (0.0065)
Top1-PB	P value	3.90×10^{-163}	5.99×10^{-181}	4.90×10^{-160}
	AUC	0.8308 (0.0024)	0.8582 (0.0298)	0.8476 (0.0192)
Autodock	P value		1.19×10^{-127}	
	AUC		0.8284	

[a]The top-scored ligand derived from the Autodock result was used for the MM/GBSA rescoring calculation.

[b]The top-scored ligand derived from the Autodock result was used for the MM/PBSA rescoring calculation.

[c]The top-scored ligand derived from the Autodock result was used for the comparison.

[d]AUC value difference calculated by $\Delta AUC = AUC_{GB/PB} - AUC_{Autodock}$.

Table II. Comparison of the rescoring accuracies of the top one docking pose and the best of the top three docking poses under different solvation models and interior dielectric constants.

AUC		ABL			ALK			BRAF			Average ΔAUC[b]
		Top 1	Top of 3	ΔAUC	Top 1	Top of 3	ΔAUC	Top 1	Top of 3	ΔAUC	
GB	ε=1	0.8475	0.8585	0.0110[a]	0.9039	0.9158	0.0119	0.8238	0.8361	0.0123	0.0117
	ε=2	0.8897	0.8932	0.0035	0.9172	0.9224	0.0052	0.8384	0.8429	0.0045	0.0044
	ε=4	0.8974	0.8997	0.0023	0.9130	0.9157	0.0027	0.8349	0.8360	0.0011	0.0020
PB	ε=1	0.7809	0.7982	0.0173	0.8297	0.8465	0.0168	0.8308	0.8493	0.0185	0.0175
	ε=2	0.8793	0.8870	0.0077	0.9105	0.9179	0.0074	0.8582	0.8657	0.0075	0.0075
	ε=4	0.8977	0.9004	0.0027	0.9137	0.9180	0.0043	0.8476	0.8517	0.0041	0.0037

[a]AUC difference between top of the three poses rescored by MM/GBSA or MM/PBSA methodologies and the top one pose derived directly from the Autodock result (also rescored by MM/GBSA and MM/PBSA approaches)

[b]Average ΔAUCs based on unique dielectric constant of the three systems.

Table III. Pearson correlation coefficients based on top of the three docking poses of MM/GBSA and MM/PBSA rescoring.

	Autodock	**GB-1**	**GB-2**	**GB-4**	**PB-1**	**PB-2**	**PB-4**
ABL	0.192[b]	0.255	0.305	0.321	0.217	0.305	0.332
Δr_{ABL}[a]	-	0.063	0.113	0.129	0.025	0.113	0.140
ALK	0.367	0.397	0.473	0.480	0.265	0.451	0.482
Δr_{ALK}	-	0.030	0.106	0.113	-0.102	0.084	0.115
BRAF	-0.182	-0.105	-0.063	-0.055	-0.170	-0.105	-0.055
Δr_{BRAF}	-	0.077	0.119	0.127	0.012	0.077	0.127

[a]Pearson correlation coefficient difference between the GB/PB accuracy and the Autodock accuracy, $\Delta r = r_{GB/PB} - r_{Autodock}$.

[b]Pearson correlation coefficient for Autodock result of ABL was calculated based on 284 known inhibitors (two known inhibitors were eliminated for the unfavorable binding score, one of 30.30 kcal/mol and the other of 727.25 kcal/mol).

Table IV. Comparison of the enrichment based on different scoring protocols (%).

Target			ABL			ALK			BRAF		
Top-scored molecules (N)			200	500	1000	200	500	1000	200	500	1000
Autodock			60.0	28.8	18.0	49.5	33.8	23.9	38.5	25.8	19.2
Minimization	GB	ε=1	57.0	31.6	18.9	61.5	43.0	27.2	41.0	30.8	21.9
			(-5.0)[a]	(9.7)	(5.0)	(24.2)	(27.2)	(13.8)	(6.5)	(19.4)	(14.1)
		ε=2	60.5	34.6	20.5	60.0	44.4	27.4	42.0	33.6	24.1
			(0.8)	(20.1)	(13.9)	(21.2)	(31.4)	(14.6)	(9.1)	(30.2)	(25.5)
		ε=4	60.0	35.8	21.2	55.5	41.6	27.7	39.5	32.6	24.3
			(0.0)	(24.3)	(17.8)	(12.1)	(23.1)	(15.5)	(2.6)	(26.4)	(26.6)
	PB	ε=1	47.5	25.4	15.6	57.0	32.6	20.6	56.5	38.2	25.8
			(-20.8)	(-11.8)	(-13.3)	(15.2)	(-3.6)	(-13.8)	(46.8)	(48.1)	(34.4)
		ε=2	60.0	33.2	19.8	59.0	40.8	26.2	54.0	37.0	25.4
			(0.0)	(15.3)	(10.0)	(19.2)	(20.7)	(9.6)	(40.3)	(43.4)	(32.3)
		ε=4	58.5	34.8	21.0	59.0	42.6	27.3	45.0	34.8	24.2
			(-2.5)	(20.8)	(16.7)	(19.2)	(26.0)	(14.2)	(16.9)	(34.9)	(26.0)
	Average		57.3	32.6	19.5	58.7	40.8	26.1	46.3	34.5	24.3
			(-4.6)	(13.1)	(8.3)	(18.5)	(20.8)	(9.1)	(20.3)	(33.7)	(26.5)
MD Simulation	GB	ε=1	57.5	34.0		63.0	43.0		42.0	34.2	
			(-4.2)	(18.1)		(27.3)	(27.2)		(9.1)	(32.6)	
		ε=2	60.5	34.6		55.5	42.2		45.0	32.6	
			(0.8)	(20.1)		(12.1)	(24.9)		(16.9)	(26.4)	
		ε=4	59.5	34.8		52.0	42.0		42.5	32.6	
			(-0.8)	(20.8)		(5.1)	(24.3)		(10.4)	(26.4)	
	PB	ε=1	52.0	32.8	-	62.5	42.8	-	53.5	35.6	-
			(-13.3)	(13.9)		(26.3)	(26.6)		(39.0)	(38.0)	
		ε=2	61.5	35.4		58.5	42.0		49.0	35.4	
			(2.5)	(22.9)		(18.2)	(24.3)		(27.3)	(37.2)	
		ε=4	60.5	35.2		53.5	42.0		45.5	34.2	
			(0.8)	(22.2)		(8.1)	(24.3)		(18.2)	(32.6)	
	Average		58.6	34.5		57.5	42.3		46.3	34.1	
			(-2.4)	(19.7)		(16.2)	(25.2)		(20.1)	(32.2)	

[a]Enrichment change ratio between the enrichment obtained from the GB/PB rescoring result and the Autodock result. The enrichment change ratio was calculated by ($Enrichment_{GB/PB} - Enrichment_{Autodock}$) / $Enrichment_{Autodock} \times$ 100.

Table V. Pearson correlation coefficients of the known inhibitors in the top 720 systems based on the minimized structures and MD simulation trajectories.

Target	Phase	GB-1	GB-2	GB-4	PB-1	PB-2	PB-4	Average	Autodock	Number
ABL	Minimization	0.33	0.39	0.40	0.29	0.39	0.42	0.37	0.09	192
	MD Simulation	0.20	0.25	0.26	0.16	0.25	0.27	0.23		
ALK	Minimization	0.16	0.25	0.26	0.18	0.26	0.28	0.23	0.24	253
	MD Simulation	0.13	0.22	0.25	0.14	0.23	0.26	0.21		
BRAF	Minimization	-0.22	-0.18	-0.15	-0.34	-0.28	-0.19	-0.23	-0.33	208
	MD Simulation	0.03	0.00	0.00	-0.16	-0.07	0.00	-0.03		

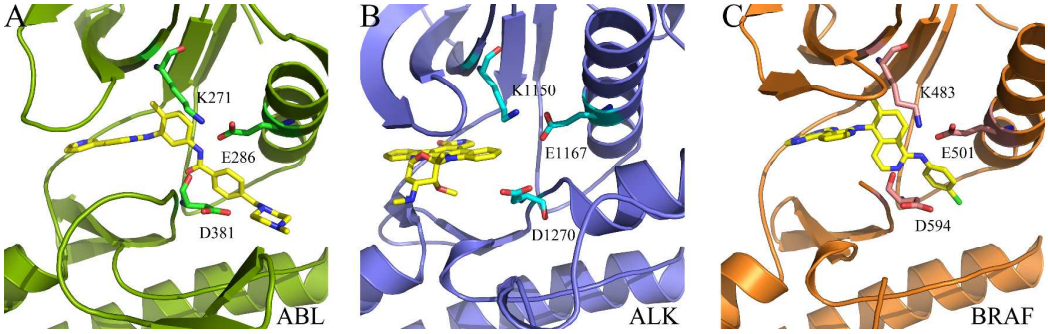

Figure 1

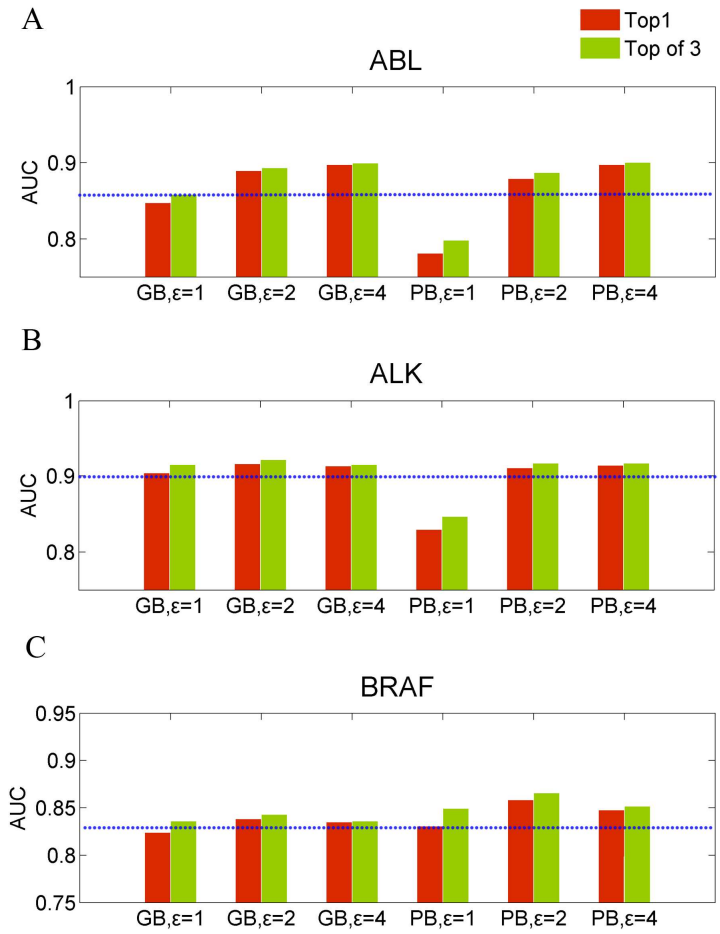

Figure 2

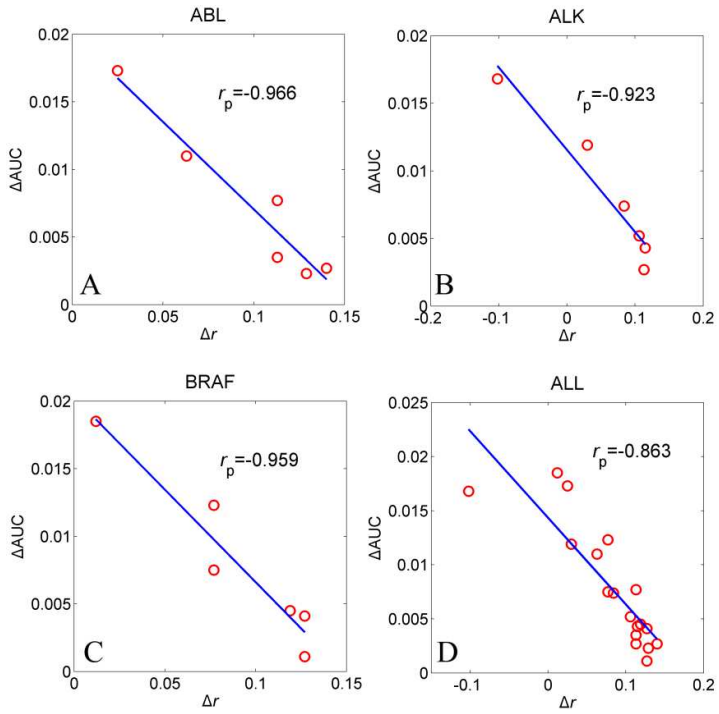

Figure 3

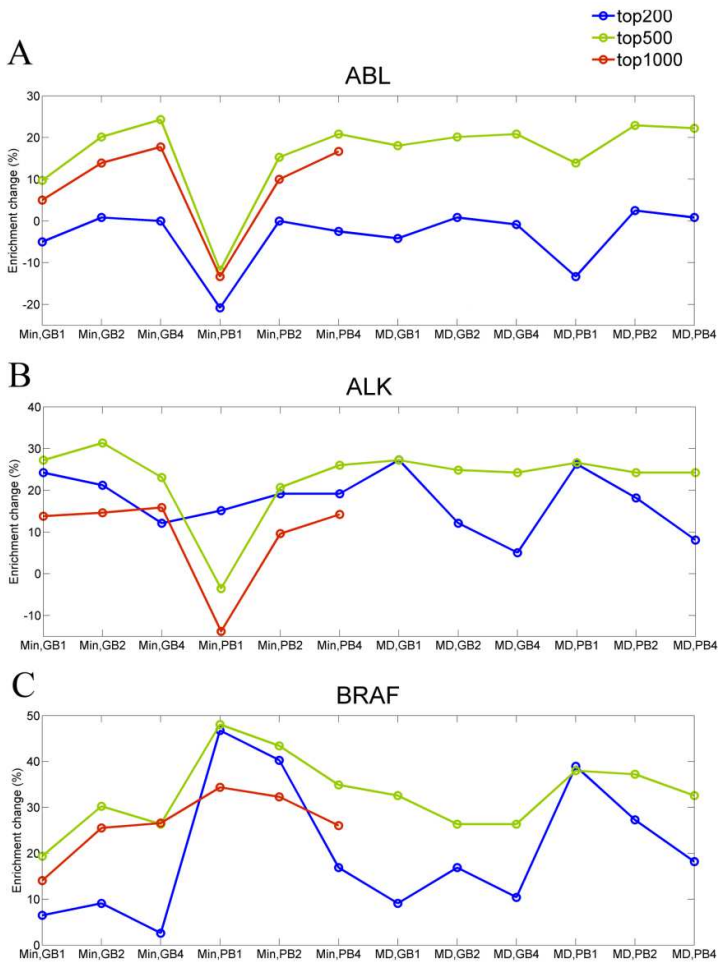

Figure 4

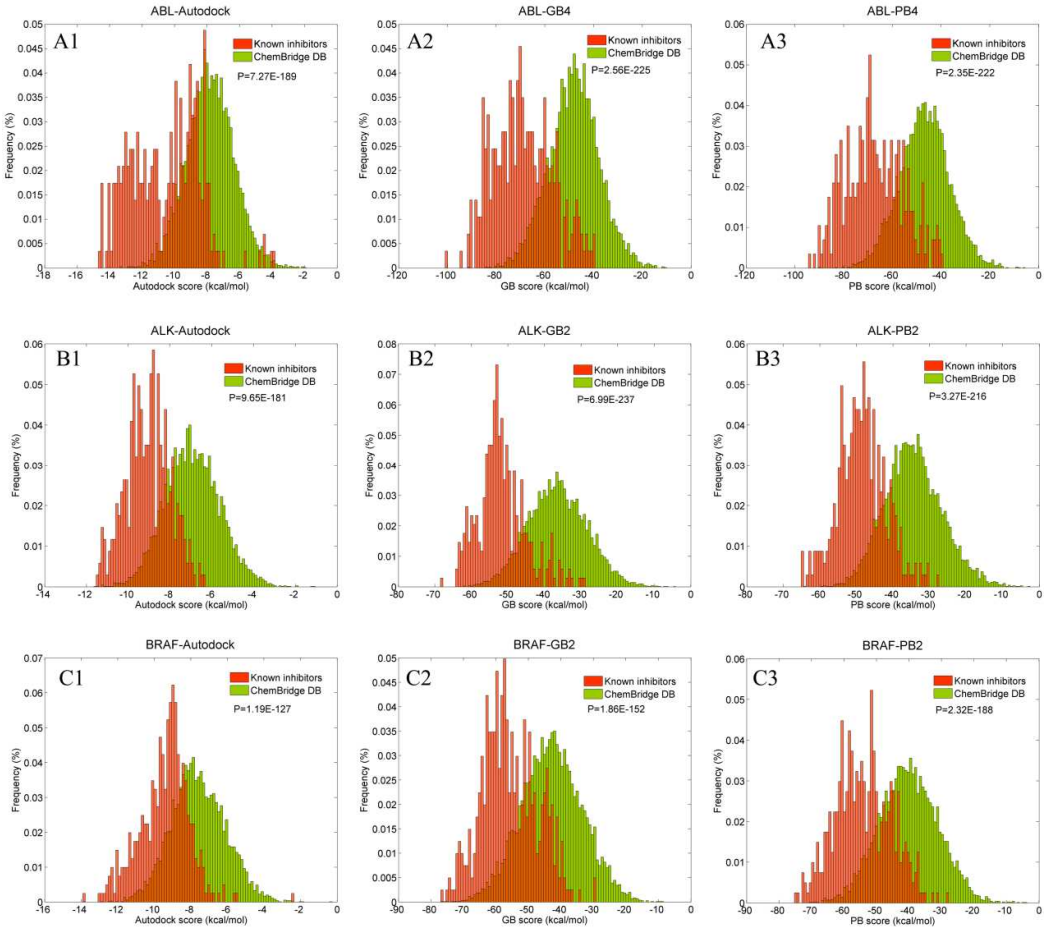

Figure 5

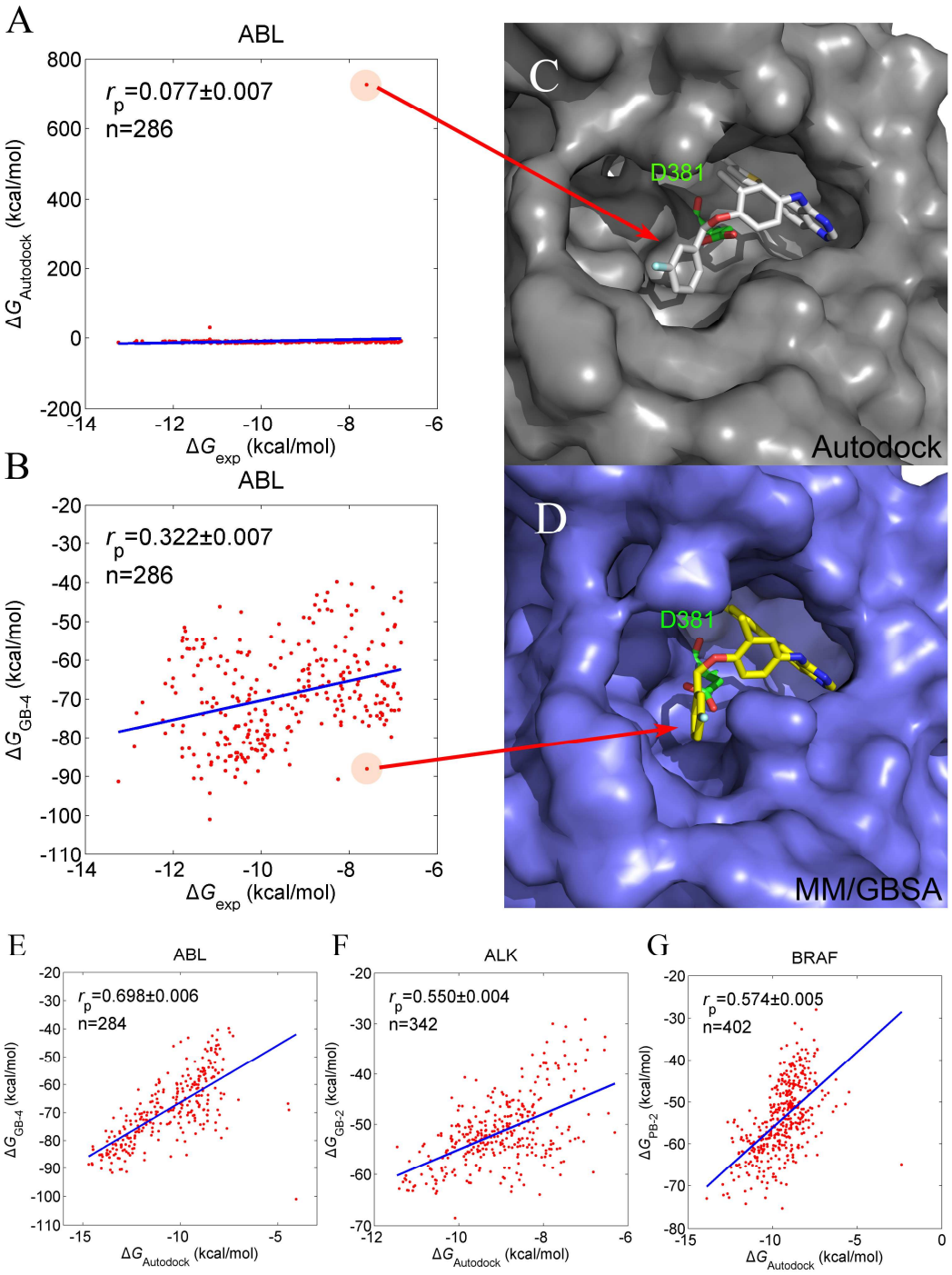

Figure 6